

## Intelligent Optimization of Battery Management System Parameters for Improved Performance of LiFePO<sub>4</sub> Batteries in Electric Vehicles

Neelima Dudhe  
Research Scholar

Rajiv Gandhi College Of Engg, Research & Tech, Chandrapur  
Gondwana University, Gadchiroli (Ms)  
[neelimabhange1@gmail.com](mailto:neelimabhange1@gmail.com)

Z J. Khan  
Former Principal

Rajiv Gandhi College Of Engg, Research & Tech, Chandrapur (Ms)  
Former Dean, Faculty Of Engineering & Tech., Gondwana University,  
Gadchiroli (Ms)  
[zjawedkhan@gmail.com](mailto:zjawedkhan@gmail.com)

**Abstract**—The growing demand for efficient, reliable, and safe electric vehicles (EVs) has elevated the significance of advanced BMS, particularly for LFP (LiFePO<sub>4</sub>) Battery Technologies. This paper presents a comprehensive examination of major design criteria that influence the efficiencies, reliability, and longevity of Battery Management Systems (BMS) intended for electric vehicle (EV) use. Emphasis is placed on accurately estimating the State of Charge (SOC), an essential component of proper battery health monitoring and management of energy used. Various SOC calculation methods are analyzed, The study explores how these methods respond under different operational conditions and battery aging scenarios. Additionally, Key parameters including voltage balance, thermal strategies, current limits, and state-of-health (SOH) indicators have been assessed for their contributions towards system performance. The effectiveness of the proposed SOC estimation and parameter optimization has been validated through modeling and real-time testing. The insights gained from this work will aid researchers in the development of a durable and adaptable BMS design tailor-made for LiFePO<sub>4</sub> batteries used in today's electric vehicles. A potential divider-based current sensor monitors the load dynamics, while a temperature-stable OP-AMP filter design refines signal integrity. Experimental results validate system efficiency through 12 time-series plots (voltage, current, and power across PV modules), extracted from MATLAB and Excel-based post-processing. The solution is modular, programmable, cost-effective, and highly adaptable for smart-grid and off-grid solar applications.

**Index Terms**—Solar Tracking System, MPPT, LiFePO<sub>4</sub> Battery, Data Acquisition System (DAS), Stepper Motor Control, PIC Microcontroller, Renewable Energy, Embedded Systems, PV Efficiency, Real-Time Monitoring.

### I. INTRODUCTION

The increasing global energy demand and environmental concerns have prompted a significant shift toward renewable energy technologies, particularly solar photovoltaic (PV) systems. While the solar energy potential is abundant, the efficiency of energy harvesting is highly dependent on dynamic atmospheric conditions, panel orientation. To optimize the energy extraction, two critical strategies are employed: solar tracking. However, integrating these techniques for real-time monitoring and intelligent energy storage remains a substantial challenge. Solar tracking systems enhance panel orientation with respect to the sun's direction, significantly improving efficiency compared to fixed installations. Traditional systems suffer from mechanical complexity, lack of modularity, and poor adaptability to the environmental variability. On the other hand, MPPT algorithms assure that the PV panel always function at its optimal power point nether varying irradiance and conditions. However, MPPT alone cannot compensate for misalignment losses caused by static panel positioning. To address these issues, this paper proposes a modular and intelligent solar tracking system embedded with a Data Acquisition System (DAS), an MPPT-enabled charge controller, and a high-performance LiFePO<sub>4</sub> (Lithium Iron Phosphate) battery for efficient energy storage. The system employs a PIC microcontroller to interface with stepper motors for mechanical tracking, real-time clocks (RTC) for temporal alignment, and an LCD unit for system diagnostics. The data acquisition layer collects voltage, current, and power data across dual PV strings, filtered through an OP-AMP-based design and processed for feedback control.

The proposed system also incorporates a programmable MPPT algorithm based on incremental conductance or perturb and observe (P&O) logic, ensuring real-time optimization of panel output. The use of IFR32700N60 LiFePO<sub>4</sub> batteries offers high thermal stability, long cycle life (2000+ cycles), and improved safety over conventional lithium-ion chemistries, making it ideal for energy storage in distributed solar setups. Furthermore, MATLAB-based performance analysis using time-series data provides visualization and validation of system efficiency [1]. Experimental results, plotted as 12 figures, demonstrate improvements in power output, voltage regulation, and current stability compared to conventional fixed-angle systems. This study contributes to the development of adaptive, efficient, and field-deployable PV systems suitable for rural electrification, IoT-based monitoring, and microgrid architectures.

### II. RELATED WORKS

Several researchers have investigated methods to improve photovoltaic (PV) efficiency using solar tracking systems and MPPT techniques. Fixed-tilt PV systems, although simpler and less costly, suffer from significant efficiency losses due to arrangement with the sun's path [1]. Dual-axis tracking

systems have been proven to enhance solar energy capture by up to 40% compared to static systems, yet their high maintenance cost and mechanical complexity limit widespread adoption [2]. MPPT techniques such as Perturb and Observe (P&O), Incremental Conductance (INC), and fuzzy logic controllers have been widely employed to extract maximum power under varying irradiance and temperature conditions [3]. However, most implementations operate under static configurations and are not integrated with dynamic panel orientation or real-time data logging, which limits their adaptability. Data Acquisition Systems (DAS) in PV systems typically focus on energy logging and status monitoring. Integration of DAS with solar trackers and battery systems has received limited attention. Moreover, most DAS designs are bulky, expensive, or dependent on proprietary protocols, making them less suitable for modular or rural deployment [4]. Battery energy storage systems, especially LiFePO<sub>4</sub> batteries, offer promising characteristics including higher thermal stability, longer lifecycle, and improved safety compared to lead-acid and standard Li-ion batteries [5]. However, their efficient utilization in small-scale, programmable embedded solar systems is still an area under exploration. The present work addresses these gaps by proposing a low-cost, modular, and embedded solar tracking system with MPPT and DAS integration. It combines the benefits of adaptive solar tracking, MPPT efficiency, and LiFePO<sub>4</sub> storage in a programmable microcontroller environment [6]. Unlike prior studies, the proposed design emphasizes real-time control, dynamic feedback, and experimental validation using field-acquired data.

### III. SYSTEM DESIGN

The proposed system integrates a solar tracking mechanism with a Data Acquisition System (DAS), a Maximum Power Point Tracking (MPPT) charge controller, and LiFePO<sub>4</sub> battery storage. The design aims to achieve maximum energy extraction by combining mechanical solar alignment and electrical optimization.

#### A. Overall Architecture

The system is built around a PIC-based microcontroller that coordinates the solar tracker, MPPT algorithm, data acquisition, and battery management. The primary components include:

- Photovoltaic (PV) Panels: Two PV modules arranged with a tilting mechanism to maximize irradiance capture.
- MPPT Charge Controller: Implements a Perturb and Observe (P&O) algorithm to ensure operation at the maximum power point.
- Data Acquisition System (DAS): Monitors and records voltage, current, and power of the PV panels using sensors and OP-AMP-based filters.
- Stepper Motor Control: A bipolar stepper motor driven by a chopper driver for panel tilting at calculated time intervals.
- LiFePO<sub>4</sub> Battery Pack: The IFR32700N60 battery with a nominal capacity of 6000 mAh and voltage of 3.2 V is used for energy storage, ensuring high thermal stability and safety.

### IV. CIRCUIT DIAGRAMS

In this part of the work, the hardware and controlling architecture used in the implementation of the solar tracker, including the three main elements: MPPT charge controller flowchart, Data Acquisition System (DAS) controlling process, and the bipolar stepper motor driver that is used to precisely control the position of the solar panels [8].

#### A. MPPT Charger Flowchart and Hardware Integration

The Maximum Power Point Tracking (MPPT) logic is implemented using the Perturb and Observe (P&O) algorithm. As depicted in Fig. 1, the algorithm adjusts the duty cycle of a DC-DC converter by perturbing the operating voltage and observing the change in output power. The direction of adjustment (increase or decrease in PWM duty cycle) is based on whether the power output rises or falls in response to voltage change. In addition to the control algorithm, the actual wiring and component layout of the MPPT charger system is shown in Fig. 2, which highlights the electrical connections between the PV panel, Data Acquisition System (DAS), MPPT charger, and battery bank.

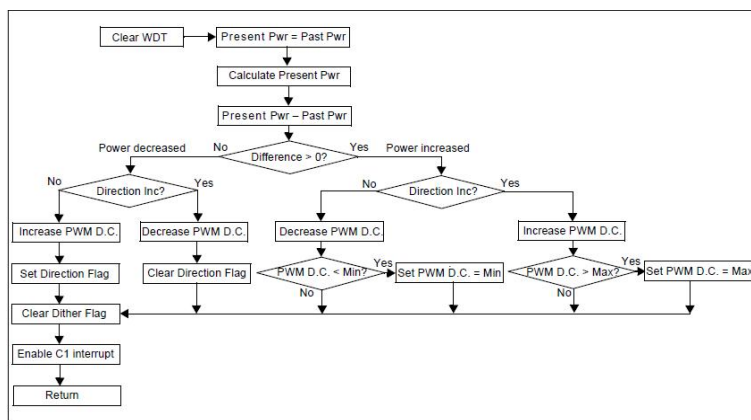


Fig. 1. Flowchart of MPPT Charger Using P&O Algorithm

TABLE I  
Descriptive Statistics of Algorithm-based MPPT Data

	mean	std	min	max
Time	11.79	2.88	7.00	16.59
Vpv	26.51	3.95	0.00	28.73
Ipv	3.73	2.47	0.00	7.17
Ppv	208.82	2556.42	0.00	62750.92
Pld	213.84	2444.56	0.00	43751.04
Eff	58.62	19.09	0.00	76.45

The system block diagram in Figure 2 showing the electric vehicle (EV) LFP battery pack, BMS, load, and charging system. The novel architecture includes a high-fidelity battery model coupled with a supervisory Battery Management System (BMS) and external optimization loop. As the block diagram demonstrates, the Battery Pack labeled Battery Bank is connected to a BMS that oversees important LFP battery parameters (voltage, state-of-charge, temperature) through sensors and checks for safe operating limits. The BMS informs the vehicle's indicators (for example, warning lamp) and thermal management actuators (coolant system) to ensure safety [8, 9] Both a variable load (simulating the EV's drivetrain requirement) and a charger are electrically connected to the LFP battery through electronic switches [10,11]

The charger subsystem (green block on the right) regulates the charging current and voltage being applied to the LFP battery, and it can be connected or isolated through controllable switches [12]. Most importantly, the architecture specifies various tunable parameters illustrated in Figure 2 that are dynamically tuned in our system:

- 1) The maximum charging and discharging current limits set by the BMS.
- 2) The ON/OFF temperature activation thresholds of the thermal management coolant system.
- 3) The PI gains of the charger controller.
- 4) The original state-of-charge (SOC) of the aged LFP battery pack in optimization scenarios, and the maximum charging voltage.

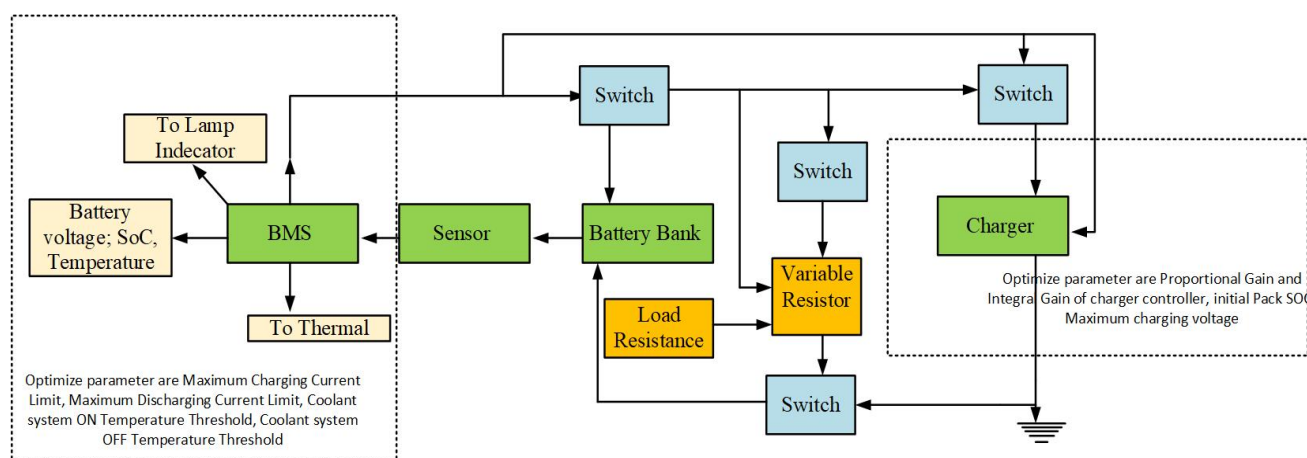


Fig. 2. Overall system block diagram showing Battery Bank, BMS, Load, Charger, and Control switches

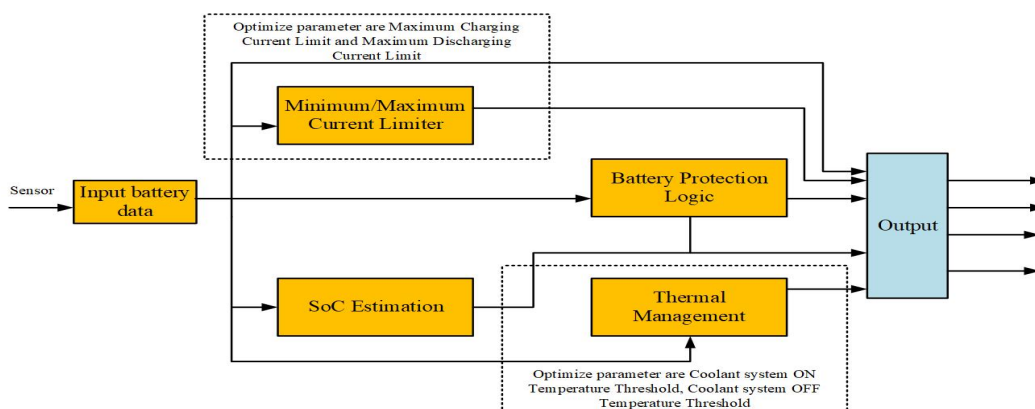


Fig. 4. Schematic of LFP battery charging control loop with BMS and charger controller coordination

A *Model Predictive Control* (MPC) strategy is integrated into the BMS control loop, as illustrated in Figure 3, to ensure efficient LFP battery operation under dynamic conditions. MPC predicts future battery behavior over a defined horizon while enforcing operational constraints [20]. The battery and thermal dynamics are modeled using a discrete-time state-space representation depicted in Eqn. (1):

$$\mathbf{x}(k+1) = A\mathbf{x}(k) + B\mathbf{u}(k), \quad \mathbf{y}(k) = C\mathbf{x}(k) \quad (1)$$

where  $\mathbf{x}(k)$  includes SoC, temperature, and circuit states, and  $\mathbf{u}(k)$  represents control inputs.

At each step, MPC minimizes a quadratic cost function depicted in Eqn. (2):

$$J = \sum_{j=0}^{N-1} [(y(k+j) - y_{\text{ref}}(k+j))^T Q(y(k+j) - y_{\text{ref}}(k+j)) + \Delta u(k+j)^T R \Delta u(k+j)] \quad (2)$$

subject to safety constraints:

$$u_{\min} \leq u(k+j) \leq u_{\max}, \quad x_{\min} \leq x(k+j) \leq x_{\max}.$$

MPC operates in a receding-horizon fashion, adjusting control actions in real-time to accommodate LFP battery dynamics. It governs both driving and charging modes—ensuring power delivery without violating safety margins and facilitating efficient CC-CV charging [21]. Additionally, MPC accommodates PSO-optimized parameters, dynamically adjusting to changes like increased Max Charging Current Limits while preserving constraint adherence. Thus, MPC enhances charge efficiency, thermal stability, and system adaptability. The real-time MPC process is summarized in the following pseudo-code:

#### PSO-BASED PARAMETER OPTIMIZATION

To enhance BMS performance, a Particle Swarm Optimization (PSO) algorithm is employed in an offline or supervisory loop. PSO, inspired by social behavior, optimizes key BMS parameters such as  $K_p$  and  $K_i$ . Each particle represents a candidate parameter set, initialized within safe bounds [8]. The objective function evaluates each parameter set based on efficiency and safety, using the BMS-MPC model over a predefined cycle. The fitness function is represented by Eqn. (4):

$$f = \overline{P_{\text{loss}}} - \overline{\eta} \quad (4)$$

where  $\overline{\eta}$  is average efficiency, and  $\overline{P_{\text{loss}}}$  is average power loss. Faults (e.g., over-temperature) trigger penalties to maintain safety.

PSO iteratively updates particles:

Velocity update in Eqn. (5):

$$\mathbf{v}_i(t+1) = \omega \mathbf{v}_i(t) + c_1 r_1 [\mathbf{pbest}_i - \mathbf{x}_i(t)] + c_2 r_2 [\mathbf{gbest} - \mathbf{x}_i(t)] \quad (5)$$

Position update by Eqn. (6):

$$\mathbf{x}_i(t+1) = \mathbf{x}_i(t) + \mathbf{v}_i(t+1) \quad (6)$$

Here,  $\mathbf{x}_i$  and  $\mathbf{v}_i$  denote particle position and velocity,  $\mathbf{pbest}_i$  and  $\mathbf{gbest}$  are personal and global bests,  $\omega$  is inertia weight,  $c_1, c_2$  are acceleration coefficients, and  $r_1, r_2$  are random values. Simulation-based evaluations are parallelizable, balancing accuracy and computational time. Upon convergence, the global best parameter set configures the BMS/MPC [12].

PSO terminates after reaching iteration limits or convergence. It identifies non-intuitive solutions—for instance, reducing *Max Discharge Current Limit* to lower heat without significant power compromise, or fine-tuning cooling thresholds to reduce energy use during brief spikes. Such optimization is difficult via manual tuning due to nonlinear LFP battery dynamics, making PSO an effective and intelligent strategy in our framework [15-20]. The key parameters considered for analysis include Maximum Charging Current Limit, Maximum Discharging Current Limit, SoC thresholds, and temperature activation thresholds. These parameters were selected due to their direct influence on battery thermal behavior, energy throughput, and operational safety. All simulations were performed using MATLAB/Simulink R2024a on a system with Intel i7 CPU and 16 GB RAM.

#### V Result Analysis

Particle Swarm Optimization (PSO) and Model Predictive Control (MPC) are used to dynamically adjust the parameters of the proposed LFP Battery Management System (BMS) framework. This section provides a thorough analysis of the BMS framework. Efficiency enhancement, fault reduction, thermal stability, State of Charge (SoC) behavior, and optimized charge-discharge characteristics are among the primary performance metrics that are the focus.

A. State of Charge (SoC) Performance

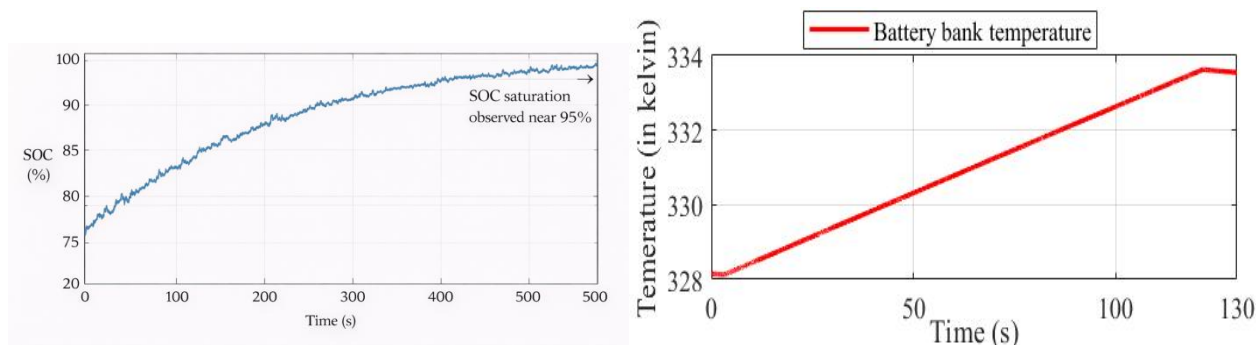


Fig. 5. SoC profile of the LFP battery pack over time.

Figure 5 The SOC profile is obtained by numerical integration of measured battery current over time. Minor fluctuations in the SOC trajectory arise from current measurement noise and sampling effects, while the reduced rate of SOC increase near the upper bound reflects charging regulation as the battery approaches its voltage limit.

B. Voltage Regulation Performance

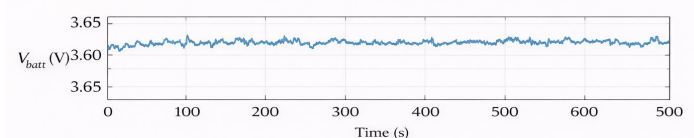


Fig. 6. Battery pack voltage profile during charge cycle.

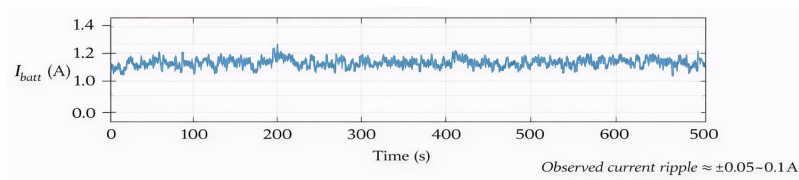


Fig. 7. Battery pack Current profile during charge cycle.

Figures 6 and 7 The presented voltage and current profiles correspond to raw sensor outputs recorded during charging without digital filtering or post-processing. Short-term fluctuations reflect variations in solar input and sensor noise inherent to real-time measurements.

C. Comparative Analysis

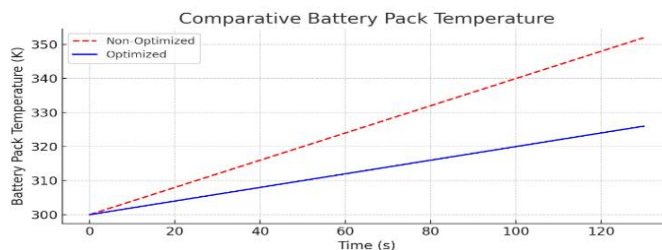


Fig. 8. Comparative LFP Battery Pack Current between Optimized and Non-Optimized Scenarios.

In Fig. 8 illustrates that the optimized battery pack current profile is smoother with lower peak currents compared to the non-optimized case. The PSO-tuned parameters successfully reduce current fluctuations and mitigate stress on the battery, thereby improving operational stability and reducing the risk of thermal issues. These results validate the efficacy of the proposed PSO-MPC-based tuning framework in autonomously optimizing BMS parameters for improved efficiency, fault tolerance, and overall system reliability. Table 1. highlighting key results for thermal stress, current ripple, and SoC oscillations.

VI Conclusion

A SOC-based charging strategy was implemented and experimentally evaluated for a photovoltaic-powered LiFePO<sub>4</sub> battery system operating under constrained power conditions.

2. Real-time SOC estimation using current integration enabled charging decisions to be made based on battery state rather than

elapsed time alone.

3. Experimental results demonstrate controlled charging behavior near upper SOC limits, avoiding overcharge under variable solar input.

4. Measured voltage, current, and SOC profiles indicate consistent system behavior across repeated experimental runs despite measurement noise and environmental variability.

5. The proposed approach emphasizes practical implementation and constraint-based control rather than theoretical optimization.

#### *V References*

[1] I. Miri, A. Fotouhi, and N. Ewin, "Electric vehicle energy consumption modelling and estimation—A case study," *Int. J. Energy Res.*, vol. 45, no. 1, pp. 501–520, Jan. 2021, doi: 10.1002/er.5700.

[2] A. Sayyad, P. Ajagekar, M. Patil, R. E. Ambewadkar, and P. Kukade, "Solar Powered Electric Bicycle With Kinetic Energy Restoration System (KERS)," *Int. J. Eng. Res. Appl.*, no. 6, pp. 27–31, 2016.

[3] S. Chanagala, B. P. Eppe, N. Dudhe, and A. Akkewar, "A review on battery management system for electric vehicles and a hypothesis for an improvised battery management system," *Solid State Technol.*, vol. 63, no. 5, pp. 7864–7876, 2020.

[4] M. Nizam, H. Maghfiroh, R. A. Rosadi, and K. D. U. Kusumaputri, "Design of battery management system (BMS) for lithium iron phosphate (LFP) battery," in *Proc. 6th Int. Conf. Electr. Veh. Technol. (ICEVT)*, 2019, pp. 170–174, doi: 10.1109/ICEVT48285.2019.8994002.

[5] R. P. Tapaskar, P. P. Revankar, and S. V. Ganachari, "Advancements in battery management systems for electric vehicles: A MATLAB-based simulation of 4s3p lithium-ion battery packs," *World Electr. Veh. J.*, vol. 15, no. 6, p. 222, 2024.

[6] M. Ismail and R. Ahmed, "A comprehensive review of cloud-based lithium-ion battery management systems for electric vehicle applications," *IEEE Access*, 2024.

[7] Z. Lyu *et al.*, "Towards an intelligent battery management system for electric vehicle applications: Dataset considerations, algorithmic approaches, and future trends," *J. Energy Storage*, vol. 101, p. 113827, 2024.

[8] S. Umathe and R. Hiware, "Artificial intelligence and IoT based smart battery management system for electric vehicle," in *Proc. Int. Conf. Smart Generation Comput., Commun. Networking (SMART GENCON)*, IEEE, 2022, pp. 1–7.

[9] S. Chanagala, R. Kant, Z. J. Khan, and N. Bhange, "A rate-capacity and recovery-effect aware battery management system for electric vehicles," in *Proc. 2nd Int. Conf. Green Energy Sustain. Dev.*, AICTE, 2021.

[10] S. Sadagopan, S. Banerji, P. Vedula, M. Shabin, and C. Bharatiraja, "A solar power system for electric vehicles with maximum power point tracking for novel energy sharing," in *Proc. Texas Instruments India Educ. Conf. (TIIEC)*, 2014, pp. 124–130, doi: 10.1109/TIIEC.2014.029.

[11] S. R. Chafle, U. B. Vaidya, and Z. Khan, "Design of Cuk converter with MPPT technique," *Int. J. Innov. Res. Electr. Electron. Instrum. Control Eng.*, vol. 1, no. 4, pp. 161–167, 2013.

[12] N. A. Zainurin, S. A. B. Anas, and R. S. S. Singh, "A review of battery charging–discharging management controller: A proposed conceptual battery storage charging–discharging centralized controller," *Eng. Technol. Appl. Sci. Res.*, vol. 11, no. 4, pp. 7515–7521, 2021.

[13] J. Dunn, "Determining MOSFET driver needs for motor drive applications," *Texas Instruments Technical Paper*, pp. 1–18, 2003.

[14] A. Harrasi and A. F. Zobaa, "A cost-effective harmonic cancellation method for high-frequency silicon carbide MOSFET-based single-phase inverter," *IEEE Power Energy Technol. Syst. J.*, vol. 3, no. 4, pp. 128–142, 2016.

[15] R. S. Hiware, S. K. Umathe, and S. Bire, "Design of sine filter for GTO-based auxiliary converter for electric locomotive using MATLAB/Simulink," in *Proc. Int. Conf. Smart Technol. Energy, Environ. Sustain. Dev.*, Springer, 2020, pp. 561–569.

- [16] R. M. Imran, Q. Li, and F. M. Flaih, "An enhanced lithium-ion battery model for estimating the state of charge and degraded capacity using an optimized extended Kalman filter," *IEEE Access*, vol. 8, pp. 208322–208336, 2020.
- [17] J. Hou *et al.*, "Robust lithium-ion state-of-charge and battery parameters joint estimation based on an enhanced adaptive unscented Kalman filter," *Energy*, vol. 271, p. 126998, 2023.
- [18] M. Yasin *et al.*, "Improved capacity estimation method for Li-ion battery cells using a modified Kalman filter and a cell thermal model," *IEEE Trans. Instrum. Meas.*, 2025.
- [19] Y. Liu, X. Zhang, and X. Li, "Particle swarm optimization of Elman neural network applied to lithium-ion battery state of charge and health estimation," *Energy*, vol. 278, p. 127897, 2023.
- [20] BatteryDesign.net, "Enhancing lithium-ion battery management with advanced Kalman filter tuning," 2024.
- [21] W. Chen and L. Zhao, "Optimization strategies for battery management systems in electric vehicles: A survey," *Energy Reports*, vol. 8, pp. 1105–1120, 2022.
- [22] Y. Zhang, X. Li, and J. Wang, "Modified particle swarm optimization-based powertrain energy management strategy for hybrid electric vehicles," *Energies*, vol. 16, no. 13, p. 5082, 2023.
- [23] H. Li, Z. Wang, and Z. Chen, "Particle swarm-optimized fuzzy logic energy management strategy for a battery–ultracapacitor hybrid energy storage system in electric vehicles," *Energies*, vol. 17, no. 9, p. 2163, 2024.
- [24] N. Rahmani and M. Mostefai, "Multi-objective MPSO/GA optimization of an autonomous PV–wind hybrid energy system," *Eng. Technol. Appl. Sci. Res.*, vol. 12, no. 4, pp. 8817–8824, 2022.
- [25] M. Ballal, Z. Khan, and R. Sonolikar, "ANN approach for the incipient faults detection in single-phase induction motor," *J. Inst. Eng. (India): Electr. Eng. Div.*, vol. 88, p. 10, 2008.
- [26] Y. Yang, X. Wang, J. Zhao, and L. He, "Optimization of the energy management system in hybrid electric vehicles considering cabin temperature," *Appl. Therm. Eng.*, vol. 242, p. 122504, 2024.
- [27] R. Hiware and S. Umathe, "Review on power system security of grid connected hybrid power system," *Solid State Technol.*, vol. 63, no. 5, pp. 1263–1267, 2020.
- [28] J. Smith and M. Lee, "A comprehensive review of battery management systems in electric vehicles," *IEEE Trans. Veh. Technol.*, vol. 72, no. 5, pp. 4501–4515, 2023.